DIFFUSIVE-ADVECTIVE GAS FLOW MODELING IN RANDOM NANOPOROUS SYSTEMS (RNPS) AT DIFFERENT KNUDSEN REGIMES

Vahid Shabro[1,2], Farzam Javadpour[2*], Carlos Torres-Verdin[1] and Sergey B. Fomel[2]
[1]Department of Petroleum and Geosystems Engineering, The University of Texas at Austin, TX, USA
[2]Jackson School of Geosciences, Bureau of Economic Geology, The University of Texas at Austin, TX, USA
*corresponding author: farzam.javadpour@beg.utexas.edu

Introduction

Determining permeability in natural fine grained porous systems such as gas-bearing shale sediments is the focus of many research activities[1,2]. Pores in these fine grained rocks are in the range of nanometers. We use the term Random Nanoporous Systems (RNPS) to address such natural systems. Gas flow in a network of nanopores deviates from Darcy flow. We introduce a systematic approach to study flow in RNPS at different Knudsen regimes.

Diffusive-Advective Gas Flow in a Nanotube

Overall equation for transport of gas molecules in a nanotube is governed by a combination of Knudsen diffusion[1] and gas flow due to pressure forces[3]:

$$J = -\left(\frac{2r}{3RT}\left(\frac{8RT}{\pi M}\right)^{0.5} + F\frac{r^2\rho_{avg}}{8\mu}\right)\frac{(p_2 - p_1)}{L} \qquad (1)$$

where J is mass flux, r is the tube radius, R is the universal gas constant, T is Temperature, M is molar mass, ρ_{avg} is average density, μ is fluid viscosity at atmospheric pressure, p_1 and p_2 are pressures at the inlet and outlet of the tube, and L in the length of the tube. The first term in the bracket is diffusive flow and the second term in the bracket is no-slip/slip gas flow due to pressure forces; F is a parameter that defines the effectiveness of slip flow on the inner boundaries and is given by

$$F = 1 + \left(\frac{8\pi RT}{M}\right)^{0.5}\frac{\mu}{p_{avg}r}\left(\frac{2}{\alpha} - 1\right), \qquad (2)$$

where, p_{avg} is the average pressure in the system, α is the tangential momentum accommodation coefficient which is the portion of gas molecules reflected diffusely from tube wall relative to specular reflection[4]. Depending on the wall surface smoothness, gas type, temperature and pressure; α varies from 0.65 to 0.85. Eq. 2 suggests that pores with smaller radii result in higher multiplier F. Lower pressure also results in higher F.

Constructing Random Nanoporous Systems

A grain pack is constructed from spherical grains and digitized using a method described in Ref. 5. Fig. 1 shows the grain pack and Table 1 describes the corresponding grain size distribution. Voxelization is performed using 200 nm grids. The connected porosity of the pack is 39.7% from 10 to 15 μm in three axes directions. (Case 1) Using the cementation method from Ref. 5, a uniform cementation process on each grain is performed to decrease the porosity to 12.4% from 10 to 18 μm in three axes directions. (Case 2)

Table 1: Summary of grain size distribution for a pack

Grain radius (μm)	Quantitative distribution	Volumetric distribution
0.5	56%	3%
1	27%	12%
2	14%	46%
3	3%	40%

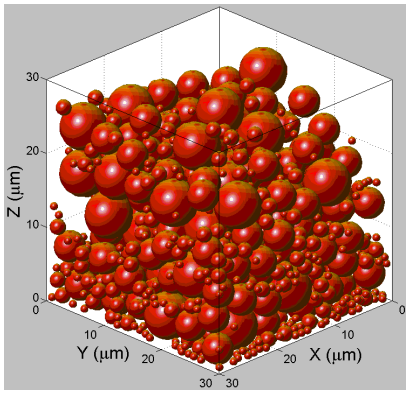

Fig. 1: The grain pack in a cubic space.

Gas Flow in Random Nanoporous Systems

At steady-state condition, a mass conserved system suggests,

$$\nabla . J = 0 \qquad (3)$$

which can be used to determine pressure distribution at any point in RNPS assuming no-flux in solid grains. Eqs. 1 combined with Eq. 2 can be written as

$$J = -\left(Ar + Br^2\right)\nabla P, \qquad (4)$$

where

$$A = \left(\frac{8RT}{\pi M}\right)^{0.5}\left[\frac{\pi\rho_{avg}}{8P_{avg}}\left(\frac{2}{\alpha} - 1\right) + \frac{2}{3RT}\right] \text{ and} \qquad (5)$$

$$B = \rho_{avg}/8\mu . \qquad (6)$$

Combining Eqs. 3 and 4, we find a modified Laplace equation in the form of

$$\nabla . d\nabla P = 0, \qquad (7)$$

where d is a weighting factor calculated for each grid according to its position in the grain pack system. The weighting factor is updated in each three Cartesian coordinate directions for all the grids to ensure a parabolic flow profile for convective dominated and no-slip flow in a tube and is calculated as

$$d_x = \left(Ar_{\max_x} + Br_{\max_x}{}^2\right) \times \frac{2d_{\max_x}d_{grid_x} - d_{grid_x}{}^2}{c_x\left(r_{\max_x}\right)} \qquad (8)$$

where r_{max} is the largest circle radius that can inscribed in the porous media perpendicular to the direction of flow that it includes the grid of interest, d_{max} is the digitized version of r_{max}, d_{grid} is the distance of the grid from the closest grain wall and $c(r_{max})$ is a calibration function included to match the flow in the digitized system with the actual flow in a tube. The average value of d in each direction between two neighboring grids is used as the weighting factor for differentiation in Eq. 7. Using Neumann's boundary condition at grain faces, and setting the actual pressure at the inlet and outlet faces, Eq. 7 can be solved to yield the pressure distribution and consequently, the mass flux distribution.

The numerical model is validated by simulating various tubes in the system. Using the parameters in Table 2, Fig. 2 shows the mass flux profile in a tube with radius of 100 nm with 25 nm grid size. The mass flux is 1.78×10^{-3} kg.m^{-2}.s^{-1} based on Eqs. 1 and 2, and 1.75×10^{-3} kg.m^{-2}.s^{-1} from the

numerical simulation. The 1.7% error is the result of digitization of the tube. Fig. 3 shows the model verification with experimental data for a nanotube with the same dimension[6].

Table 2: Summary of simulation parameters.			
r (nm)	100	R (J.kmol^{-1}.K^{-1})	8310
T (K)	300	M (kg.kmol^{-1})	39.94
α	0.8	Δp (Pa)	1
μ (Pa.s)	2.22×10^{-5}	L (nm)	300
ρ_{avg} (kg.m^{-3})	2.85	*Grid size* (nm) [tube]	25
P_{avg} (Pa)	164000	*Grid size* (nm) [pore]	200

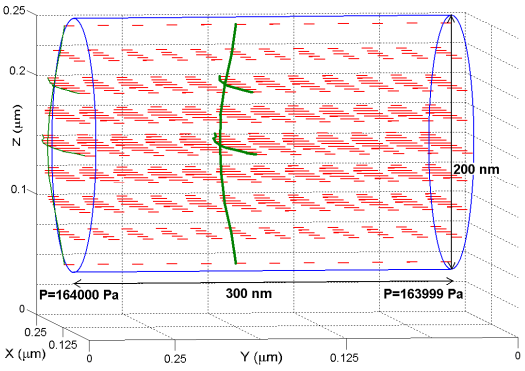

Fig. 2: Gas flow in the tube. The parabolic flow profile is highlighted with the green line.

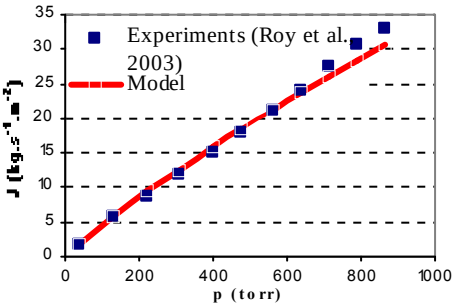

Fig. 3: Model prediction *vs.* experimental data

Results

Cases 1 and 2 for porous media are modeled using the aforementioned method and the parameters listed in Table 2. The corresponding permeability is calculated using Darcy's law. Table 3 shows the corresponding simulation results.

Fig. 4 shows the flux profile for case 1 and a pressure profile at a cross-section of the system. Fig. 5 illustrates the effect of P_{avg} for case 1 on the mass flux. Variations in average pressure end in transformation in various Knudsen transport regimes as it is evident from Eqs. 1 and 2.

Table 3: Summary of simulation results and relevant permeabilities.		
Parameters	Case 1	Case 2
J (kg.s^{-1}.m^{-2})	1.12×10^{-2}	2.13×10^{-3}
V (m^3.s^{-1}.m^{-2})	3.95×10^{-3}	7.49×10^{-4}
Φ	39.70 %	12.40 %
Δp (Pa)	1	1
L (m)	5×10^{-6}	8×10^{-6}
μ (Pa.s)	2.22×10^{-5}	2.22×10^{-5}
K (md)	444	135

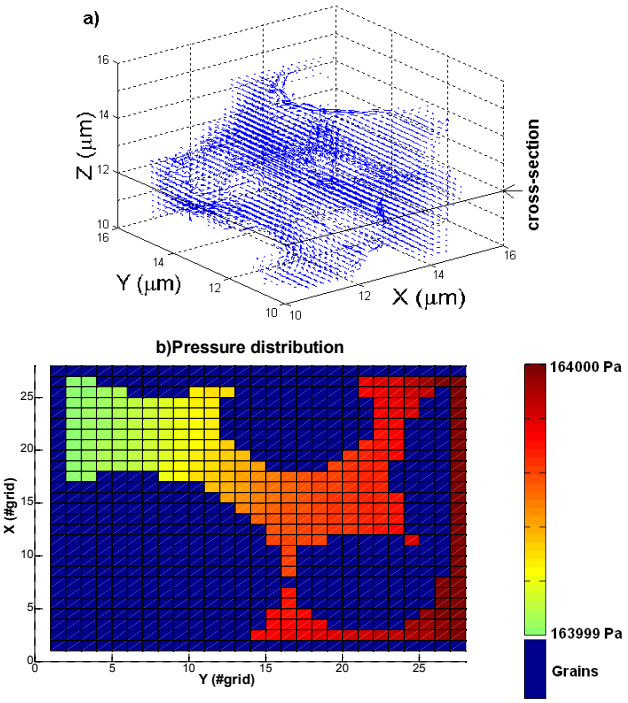

Fig. 4: (a) Flux distribution for case 1. (b) Pressure distribution at z = 12 μm

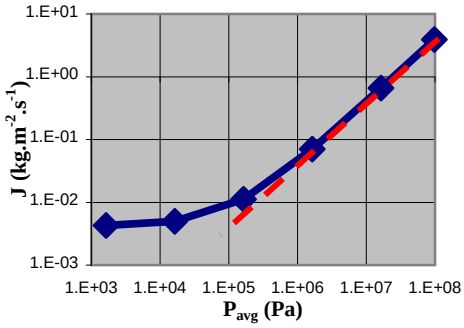

Fig. 5: Flux variations vs. P_{avg}, transition for different Knudson transport regimes using simulations for Case 1.

Conclusions

1. We developed a gas flow model which implements both diffusion and advection transports in random nanoporous systems using a modified Laplace equation.
2. The model was implemented for three cases. We illustrated the existence of various Knudson transport regimes in random nanoporous systems.

References

1. Javadpour *et al.*, "Nano-scale gas flow in shale sediments" *J. Can.Petrol. Tech., 46:10, p.55–61(2007)*
2. Katsube, T.J. "Shale permeability and pore-structure evolution characteristics" *Current Research 2000-E15, Geological Survey of Canada, Ottawa, ON (2000)*
3. Bird *et al.*, "Transport Phenomena" 2nd edition, *John Wiley & Sons, Inc. (2007)*
4. Maxwell, J.C., "The Scientific Papers of James Clerk Maxwell" *Cambridge University Press, V.2, p.708 (1890)*
5. Silin *et al.*, "Robust determination of the pore space morphology" *SPE 84296 (2003)*
6. Roy *et al.*, "Modeling gas flow through microchannels and nanopores" *J. Appl. Physics, 93:8, p.4870-4879 (2003)*

This project was jointly funded by Advanced Energy Consortium & UT Austin's Research Consortium on Formation Evaluation.